Iranian Journal of Geophysics, Vol. 9, No. 5, 2016, Page 24-39

Classification of hydrometeors using microwave brightness temperature data from AMSU-B over Iran

Abolhasan Gheiby[1*] and Majid Azadi[2]

[1]*Assistant Professor, University of Hormozgan, Bandar Abbas, Iran*
[2]*Associate Professor, Atmospheric and Meteorological Research Centre, Tehran, Iran*

(Received: 4 March 2014, accepted: 10 March 2015)

Abstract

The Advanced Microwave Sounding Unit-B (AMSU-B) installed on the NOAA-15, 16, and 17 satellites, is the new generation of a series of microwave imagers/sounders that can sense atmospheric moisture and other hydrometeors through clouds. This paper demonstrates the potential of multi-frequency AMSU-B data for classifying different types of hydrometeors. Ten types of these hydrometers have been collected using meteorological data (synoptic reports, radiosonde data and infrared and water vapor images) over Iran. Co-located AMSU-B data were used to perform a quantitative classification of the hydrometers. Three main classes including heavy precipitating, moderate precipitating, and non-precipitating hydrometeors were found based on the multi-frequency brightness temperature signatures. The distinguishing criteria for this type of analysis are: (a) brightness temperature (BT) at 89 GHz frequency, (b) slopes of the BT between 89 and 150 GHz, and (c) crossover of BT curves between 89 and 183 GHz frequencies.

Keywords: Classification, AMSU-B, hydrometeors, brightness temperature

1 Introduction

In line with the advances in visible (VIS) and infrared (IR) remote sensing for observing weather phenomena, the usage of observations with the help of the microwave (MW) portion of the electromagnetic spectrum (all using low earth orbiting satellites) has also been developed (Kidder et. al. 2000). Compared to satellite-visible and infrared measurements that only sense the top portion of clouds, microwave measurements are very useful for probing precipitation, as they sense hydrometeors through the entire cloud and precipitation layer.

*Corresponding author: abolhassang@yahoo.com

There have been several studies related to hydrometeor remote sensing. Liu and Curry (1996, 1997) studied the large –scale cloud and precipitation features in the North Atlantic using satellite microwave data. They developed an ad hoc snowfall algorithm using high-frequency microwave data for partitioning the total precipitation into rain and snow. Schools et al. (1999) studied snowfall signatures associated with a North Atlantic cyclone. They emphasized the different responses of 85 GHz microwave radiation to the cumulonimbus portion along the squall line and the nimbostratus portion north of the low-pressure center. Katsumata et al. (2000) studied snow clouds over the ocean using a radiative transfer model and observations from an airborne microwave radiometer and an X-band Doppler radar. Bennartz and Petty (2001) investigated the effect of variable size distribution and density of precipitating ice particles on microwave BT and noticed that the radiation between scattering indices and precipitation intensity might systematically vary with the types of precipitation. Wang et al. (1997) studied storm-associated microwave radiometric signatures in the frequency range of 90-220 GHz. However, most of the earlier microwave sensors had a coarse resolution. High spatial and temporal resolutions, depending on the meteorological phenomena under consideration, are generally required to define the atmospheric meso-scale phenomena.

The Advanced Microwave Sounding Unit-B (AMSU-B) is a cross-track scanning microwave sensor with channels at 89, 150, 183.31 ± 1.00, 183.31 ± 3.00, and 183.31 ± 7.00 GHz (Saunder et al. 1995; NOAA KLM User's Guide, available at: http://www.2.ncdc.noaa.gov.docs/klm). These channels are called channels 16 to 20 of the overall AMSU instrument. Channels 1 to 15 belong to AMSU-A. The instrument has a swath width of approximately 2300 km, which samples at 90 scan positions. The satellite viewing angle for the innermost scan position is about 0.55º from nadir, for the outermost scan position, it is 48.95º from nadir. These correspond to an incidence angle of 0.62º and 58.5º from nadir, respectively. The footprint size is 20 × 16 km^2 for the innermost scan position, but increases to 64 × 52 km^2 for the outermost scan position. The AMSU-B data for this study was obtained from the Comprehensive Large Array-data Stewardship System (CLASS) of the US National Oceanic and Atmospheric Administration (NOAA). Some related meteorological applications of the AMSU data were also exemplified in researches related to study of tropical cyclones (Kidder et al. 2000), precipitation characteristics over land (Ferraro et al. 2000), determination of total perceptible water and cloud liquid water over Ocean (Grody et al. 2001), and precipitation observations near 54 and 183 GHz (Staelin et. al. 2000). To further explore the application of microwave data for all weather signatures, this study was concerned with the quantitative AMSU-B measurements for different types of precipitating and non-precipitating hydrometeors as well as snow cover in the mid-latitudes, represented for Iran. Through this study, we attempted to answer the questions: What is the

sensitivity of radiation at various frequencies with respect to specific hydrometeors? What is the optimal frequency or combination of frequencies to detect different types of hydrometeors?

In this paper, after indicating the study area in section 2, the sources of our data and procedures of selecting proper data for further analysis are explained in sections 3 and 4, respectively. The methodology of measurements and quantitative microwave BT signatures, with respect to different types of hydrometeors viz.: (i) Heavy precipitation hydrometeors (thunderstorms and heavy rain), (ii) Moderate and low precipitation hydrometeors (moderate and light rainfall as well as snowfall) and (iii) Non-precipitation hydrometeors (moisture and cloud at different atmospheric levels, such as low-level moisture, upper-level moisture), along with clear sky and snow-covered conditions are explained in section 5.

In section 6, the classifications of hydrometeors which belong to three main classes are investigated using quantitative microwave BT signatures at different frequencies of AMSU-B channels. The trend microwave signature namely channel versus BT, is related to the height variation of moisture and hydrometeors at any selected spot/station. The signatures of the above mentioned three classes, in AMSU-B data, are described in more details and discussed in section 7. A case study of some hydrometers and conclusions are presented in sections 8 and 9.

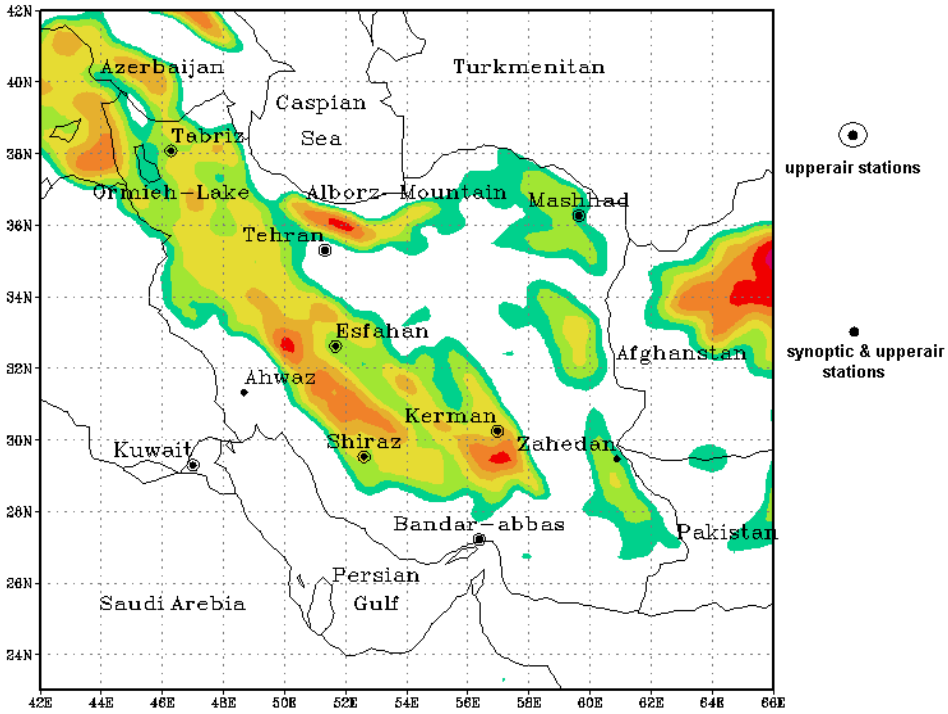

Figure 1. Geographical map of Iran along with cities from which data have been collected.

2 Study area

In this study, data have been collected over Iran (23-45 N, 45-65 E), which is located in the Middle East. Figure 1 shows a geographical map of Iran and the location of the stations, from which data have been collected. As it is seen, the stations are distributed almost evenly over the country.

3 Data Sources

Two sets of data including ground base and satellite data were used in the analysis:

(A) Ground base data included seven surface weather phenomena (Thunderstorm (TS), Heavy Rain (HR), Moderate Rain (MR), Light Rain (LR), Snowfall (SF), Snow Cover (SC), and Clear Sky (CS)) and three upper level conditions (Moist Low level (ML), Moist Upper-level (MU) and Dry Upper level (DU)) extracted from hourly synoptic reports and radiosonde observations respectively (Table 1).

(B) The satellite data is used as the second data-set. The visible and infrared images are taken from METOSAT satellite (available online at: http://www.sat.dundee.ac.uk) and the microwave level 1b data from AMSU-B onboard the National Oceanic and Atmospheric Administration (NOAA) polar-orbiting satellites (available online at: http://www.class.noaa.gov).

Presently, eight passes of AMSU-B data per day are available (four satellites carry AMSU-B instruments and each satellite can view twice a day any geographical location). As an example, Table 2 gives the flyover time of three NOAA satellites over the study area (Iran). AMSU-B instruments contain the observed thermal emissions at several frequencies near 183 GHz, strong water vapor line, along with a window channel at 89 GHz, and one intermediate channel at 150 GHz.

TABLE 1. Meteorological weather events (in abbreviated forms) and corresponding number of reporting stations.

No.	Events	No. Reports	No. AMSU-B selected pixels	No.	Events	No. Reports	No. AMSU-B selected pixels
1	Clear Sky(CS)	28	250	6	Heavy Rain (HR)	14	140
2	Snow Cover (SC)	20	200	7	Snow Fall (SF)	15	150
3	Low level Moisture (LM)	15	150	8	Thunderstorms (TS)	12	120
4	Light Rain (LR)	22	200	9	Upper level Moisture (UM)	150	150
5	Moderate Rain (MR)	23	200	10	Upper level Dry (UD)	150	150

TABLE 2. Flyover times of NOAA satellites for Iran. The capital letters N and S indicates North and South respectively.

Satellites	NOAA16 N → S	NOAA15 N → S	NOAA17 N → S	NOAA16 S → N	NOAA15 S → N	NOAA17 S → N
Time passes	~12PM	~03AM	~09AM	~12 AM	~03PM	~09PM

The AMSU-B level 1b data contain radiometric calibrated BTs, and their corresponding earth locations. The limitation for this data-set is its short time coverage over study area that is less than 30 minutes per day (~ 7 minutes per passes).

4 Data selection procedures

Clear sky weather condition and surface covered with snow were extracted from collocated visible/infrared METEOSAT data. Radiosonde observations are used to extract the moisture conditions at different altitudes and are referred to as ML, MU and DU in Table 1. It is to be noted that ML conditions for a specific location means that the RH up to 700 hPa is more than 70% and UM refer to places with RH more than 50% above the 500 hPa level. DU means RH less than 20% above the 500 hPa level.

For the synoptic reports showing TS, different types of rain (HR, MR, and LR), and SF at a specific time, the corresponding AMSU-B data within a time interval were collected. The time interval was less than 10 minutes for TS and HR, less than 30 minutes for MR, LR, SF, and less than 1 hour for MU, ML, and DU. It should be noted that rapidly developing TS may have significantly changed their state within the short time frame considered, since the time difference between the synoptic reports and the AMSU-B passes, for TS cases, was at most 10 minutes. The events in Table 1 correspond to a total of 183 synoptic station-reports and about 150 passes of AMSU-B, corresponding to the reports available. The BT values of 1710 pixels, close to the synoptic reports, for 183 stations were used (Table 1). The stations are distributed over different locations of Iran (Figure 1), and the events took place during different days from May 2001 to October 2002. Some types of the events, such as HR, TS and SF had lower frequencies over Iran region.

5 The measurements

The upwelling microwave radiation reaching the AMSU-B sensors results from the atmosphere, clouds and surface contributions. These contributions are made up of complex interactions including emission, absorption, and scattering by water vapor, water droplets, and ice crystals in the clouds, as well as by ocean and land surfaces. Therefore, radiance $(B_\nu(T))$ at top of the atmosphere, which is measured by the satellite, is an integrated effect of the contributions from all of these interactions (Muller et al 1994).

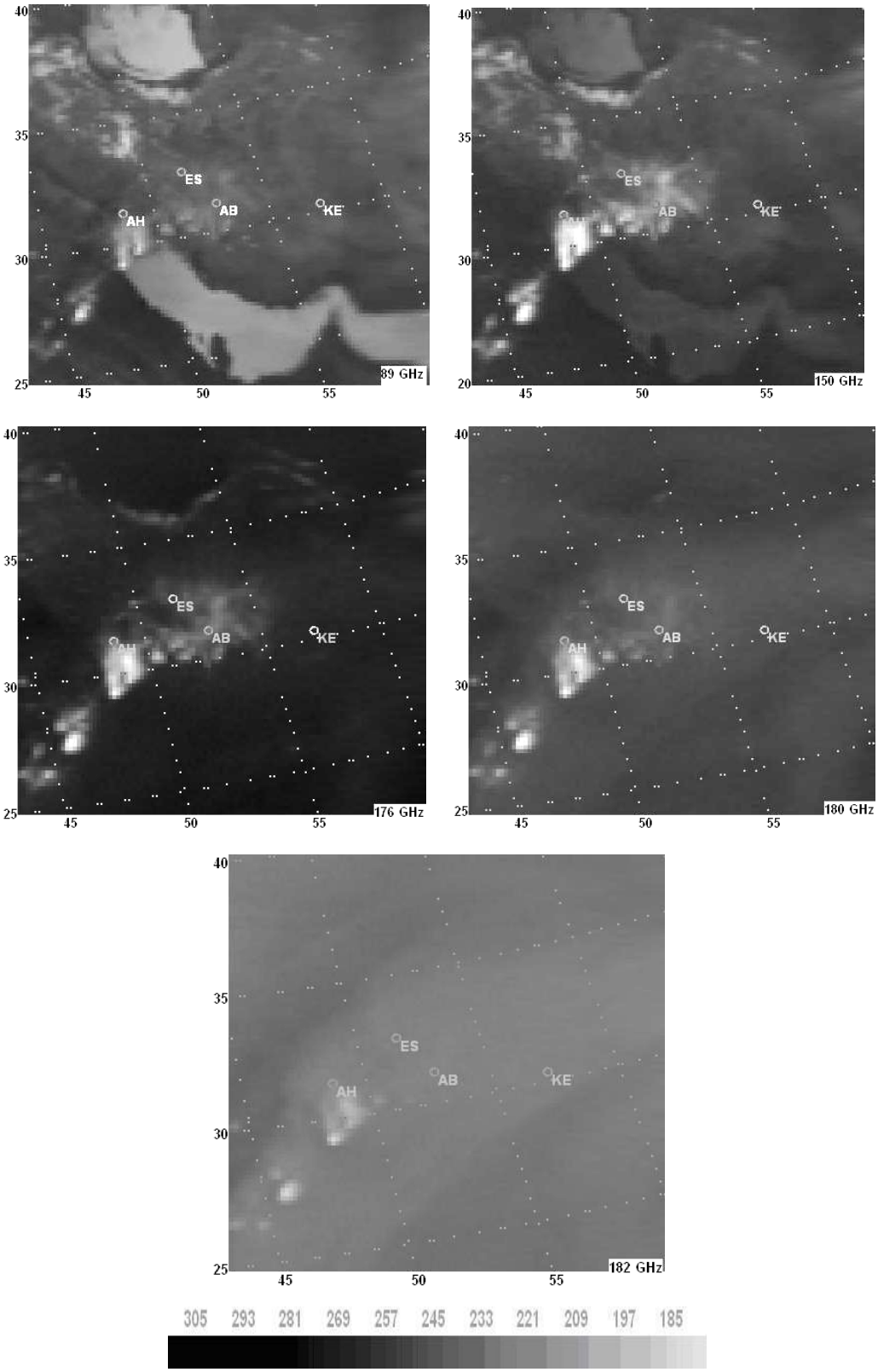

Figure 2. Five images of AMSU-B channels on 07 December 2001 at 2250 GMT along with the corresponding scale of BTs in Kelvin. Longitudes and latitudes are indicated by dotted lines.

AMSU-B level 1b data is the radiance that is converted to BT, and is available from the Large Array-data Stewardship System (CLASS. The AMSU-B images of one pass, as an example, are given in Figure 2, which shows four meteorological phenomena viz. (1) TS (Ahwaz), (2) HR (Abadeh), (3) MR (Esfahan), and (4) CS (Kerman), for 08 December 2001 at 2250 GMT. To study the properties of AMSU-B frequencies in regions covered with snow, data for the Alborz Mountain, in clear sky conditions, during winter season were used. The Alborz Mountain, with the maximum height of 5600 m, is located in the north of Tehran (Figure 1); it is always covered with snow from November to April. The clear sky conditions were recognized from METOSAT images. For selecting the events, we first examined the corresponding synoptic reports. The geographical position of each event was located in all the five AMSU-B images. Then, the BTs of several pixels (~10 pixels per report) over five AMSU-B images were calculated. Finally the BT was averaged over all reports for each specific event. To classify the hydrometeors, BT variation and average BT versus frequency-channels for different hydrometeors were presented in Figure 3 and Table 3.

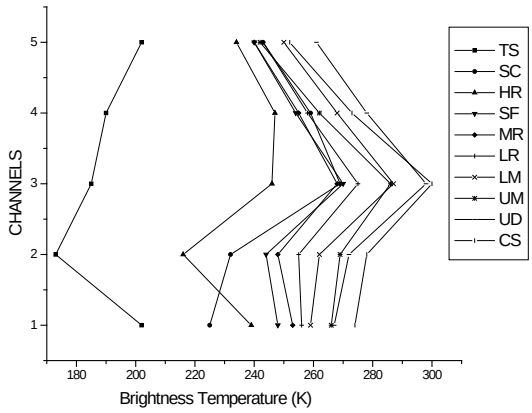

Figure 3. The average values of BTs as a function of frequency-channel for all hydrometeors. Numbers 1 to 5 on the vertical axis correspond to channels 16 to 20, respectively.

Figure 3 shows that the BT curves for each specific event are sufficiently different from each other. Therefore, these curves can be considered as multi-spectral

TABLE 3. Average values of BT for all hydrometers over all stations.

Fr.(GHz)	CS	SC	UD	UM	LM	LR	MR	SF	HR	TS
89	274±10	225±10	267±6	266±8	259±7	256±6	253±6	248±7	239±7	202±25
150	278±9	232±9	272±6	269±8	262±8	255±8	248±10	244±8	216±9	173±20
176	300±6	269±8	298±5	286±4	287±9	275±6	268±8	270±7	246±6	185±21
180	273±5	259±4	278±4	262±3	268±8	258±5	255±5	254±3	247±4	190±24
182	252±5	243±6	261±4	242±3	250±8	243±7	240±4	240±3	234±3	202±24

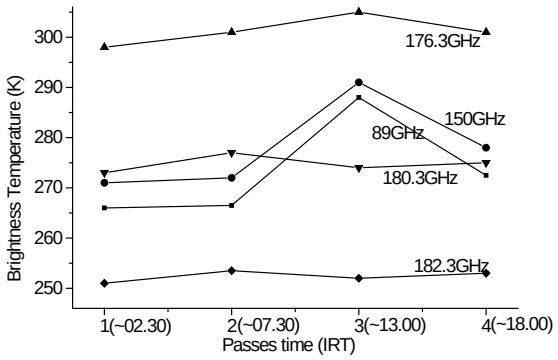

Figure 4. The BT variations for five AMSU-B frequencies (channels) for different passes over Iran region.

microwave signatures for different types of hydrometeors. However, there are several "not clearly separable" cases, which are discussed below in more details. The most notable ones are the differences between dry and wet surfaces, the effect of snow cover, and the time of day for data recording. Dry surfaces tend to have the highest emissivity and BTs, while, the wet surfaces and surfaces with snow cover tend to have the lowest emissivities, and therefore, have lower BTs when compared to dry lands. The observed BT variability over homogenous land was due to the variations in land surface temperatures and surface emissivities. As stated above, in clear sky conditions, the time of the day for data gathering is also an important factor that affects the BT in the lower frequencies of AMSU-B (89 and 150 GHz). This effect is shown for different passes in Figure 4. This is due to the higher values of the radiance weighing functions at and near the earth surface for these channels. During the afternoon, when the earth surface and its lower atmosphere get warmer, the BT at lower frequencies increases (Pass 3 in Figure 4). During the night and early morning, when the earth surface was cooler, the BT decreased (Passes 1 and 2 in Figure 4). The 176-182 GHz frequencies were not much affected by the time of the day for data collection, because a maximum contribution to the BT for these frequencies comes from 790 hPa (~ 2 km above ground) and above (Muller et. al. 1994), which is not generally much influenced by the time of the day.

6 Classification of hydrometeors and signatures indications

The signatures of different hydrometeors, presented in Table 1, are different from each other as stated above (Figure 3). The range of BT for thunderstorm was larger at all frequencies (Table 3). For example, this range was 81 K (145-226K) at 89 GHz and 71 K (151-222 K) at 182.3 GHz, whereas for ML, it was only 16 K (249-265 K) at 89 GHz and 30 K (237-267 K) at 182.3 GHz.

Figure 3 also indicates that some classes are relatively well separated only at several specific frequencies, e.g. HR with BT between 200 and 220 K at 150 GHz. It is obvious that discrimination between all of the hydrometeors could not be accomplished from five AMSU-B BTs only. However, through a combination of two (or more than two) BT channels, these classes may become distinguishable. For example, SC can be distinguished from other hydrometeors by combining 89 and 176.3 GHz frequencies. SC was very cold at 89 GHz (BT less than 225 K), whereas it was warm at 176.3 GHz (BT values higher than 255 K (Figure 3)). Note that this was

not the case for other hydrometeors. Considering the BT values at 89 GHz and 150 GHz, the hydrometeors can be conveniently classified into three major classes: (i) Heavy precipitation and snow cover class (TS, HR and SC), (ii) Moderate precipitation class (LR, MR, and SF), (iii) Non-precipitating class (LM, UM, UD, and CS).

6.1 Heavy precipitation hydrometeors

The Class I, which is considered as heavy precipitation hydrometeors, includes TS, HR and SC which have the coldest BT at 89 and 150 GHz. Their multi-frequency signatures are more clearly presented in Figure 5. For example, the highest BT value in this class (at 89 GHz), which is related to HR, is about 243 K and the lowest one, which is related to TS, is about 145 K (Figure 5). At 150 GHz, the highest value of BT, for this class, is about 240 K (related to SC), and the lowest one is around 125 K (related to TS). While TS and HR are still separable at 150 GHz, but SC is mixed up with the second class (Figure 3). The 150 GHz frequency shows a lower BT for TS and HR, because TS and HR are mostly comprised of large water droplets and ice particles at the mid-level of the troposphere, which scatter microwave at low frequencies. However, at frequencies 176.3 GHz and above, the BT curves for HR and SC are converged to similar values for Classes II and III. Note that TS is clearly separable at all five AMSU-B frequencies. For frequencies above 150 GHz, HR and SC are following similar variations of BT, except that HR is shifted to colder values by ~10K. Between 89 and 150 GHz, HR and SC have a cross over; BT(89) > BT(150) for HR, and BT(89) < BT(150) for SC. From average BT curves, it can be seen that the signature differences, for this class, are very clear at 176 GHz (Figure 3). At higher frequencies, BT curve for TS has an opposite trend when compared with SC and HR, such that it is continually increasing at all frequencies above 150 GHz. This is while for SC, the value of BT from 89 to 176 GHz, increases and from 176 to 182 GHz it decreases. BT curve for HR at frequencies above 150 GHz shows a similar trend as SC does except that for HR from 176 to 180 GHz there is a slight increase. It should be noted that the hydrometers in this class are obviously separated from each other at 176.3 and 180.3 GHz

6.2 Moderate precipitating hydrometeors

The SF, MR, and LR, which comprise the medium intensity precipitating hydrometeors, belong to Class II. This class of hydrometers has a moderate BT and a minor positive slope for the TB

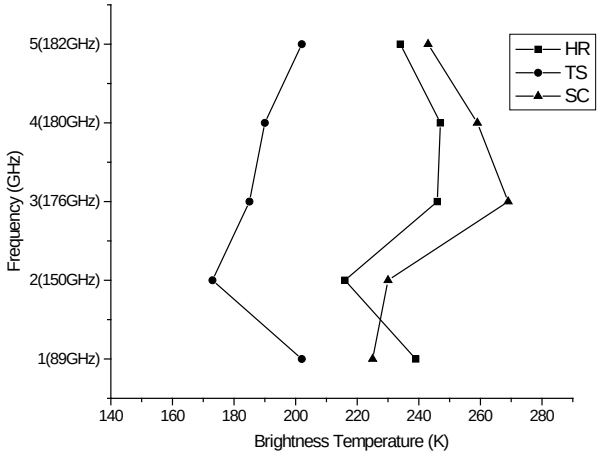

Figure 5. The average values of BT as a function of frequency-channel for heavy precipitation hydrometeors and snow cover (TS, HR, and SC).

curve between 89 and 150 GHz (Figure 3). Since moderate precipitating hydrometers mostly occur at mid and low levels of the troposphere, their BT curves all have negative slopes between 89 and 150 GHz, i.e. BT (150 GHz) < BT (89 GHz). Their multi-frequency mean variations, i.e. signature curves (along with LM signature curve), are presented in expanded form in Figure 6. It can be seen from Figure 6 that moderate precipitating hydrometeors are not as clearly differentiable as heavy precipitating hydrometeors in Class I. The BT value for 150 GHz is at most 5 K colder than its value at 89 GHz for MR and only 1 K colder for LR (Table 3). All hydrometers of this class have similar ranges for BT at all frequencies. For example, the highest BT value at 89 GHz is about 266 K and the lowest BT is about 235 K. The 150 GHz frequency also has a similar range, e.g. the highest BT value at 150 GHz, is about 262 K, and the lowest BT is around 232 K and average BT for 176.3 GHz is limited between 255 and 280 K. Some reasons for the similarities and dissimilarities of hydrometers in Class II may be pointed out. In SF, the BT is depressed due to scattering loss by ice particle and reaches average values of approximately 248 and 244 K at 89 and 150 GHz, respectively. An increase in the average BT at 89 GHz for LR (256 K) and MR (253 K) may be due to emission from water vapor at the low levels of the troposphere. Similarly, the slight decrease in BT from LR to MR may be due to scattering loss by larger water droplets in the MR. The reason for a similar response of water vapor channels (176-182 GHz) to MR and SF is due to the fact that in our region of study (Iran) rain almost occurs in the form of cold rain (with a layer of ice crystals aloft). Signatures of SF and MR have maximum ambiguity. The only distinctive point is that their respective BT curves cross over at lower and higher altitudes, i.e. $BT(150)_{SF} < BT(150)_{MR}$ and $BT(176)_{SF} > BT(176)_{MR}$, whereas $BT(182)_{SF}$ and $BT(182)_{MR}$ converge to similar values.

6.3 Non-precipitating hydrometeors

The Class III, includes non-precipitating hydrometeors (LM, UM, UD, and CS) which has the highest BT and a negative slope for the BT curve between 89 and 150

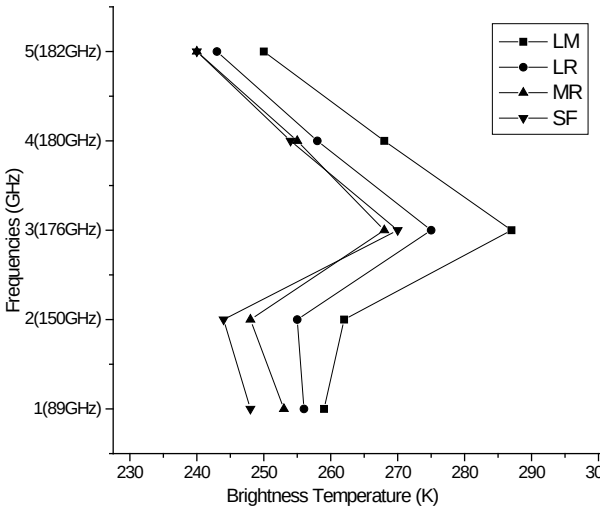

Figure 6. The average values of BT as a function of channel-frequency for hydrometeors in Class II: LR, MR, and SF along with LM as a reference.

GHz. The multi-frequency signatures of these non-precipitating hydrometers are more clearly presented in Figure 7. The average BTs for this class are the highest compared to both Class I and II and have a wide range, between 255 and 295 K, at 89 GHz. The BT related to these hydrometeors show a slight rise from 89 to 150 GHz, and then a major rise up to 176.3 GHz, followed by a continuous fall, up to 182.3GHz.

From Figure 7 it can be seen that the hydrometeors of this class (except LM, which is mixed up with LR from Class II) can be clearly separated from Class II, because their respective curves show higher BT at all frequencies. The BT at 176.3 GHz is less than 275 K for Class II ($BT\ (176)_{II} < 275$ K), whereas for Class III it is higher than 280 K ($BT(176)_{III} > 280$ K). It can also be seen, that in general, the BT curves are not clearly separated from each other (Table 3). However, some points may be noted for average values of BTs: As in the case of SF and MR in Class II, the LM-UM and UD-SC BT curves give an ambiguous signature, because at 176.3 GHz, they differ from each other by an amount less than their respective range (Table 3). Despite nearly the same BT at 89 and 150 GHz, for UD and UM, the BT signatures are remarkably different at frequencies near 183 GHz. The reason for this is that scattering by ice particles causes an almost linear decrease in BT up to only 263 and 243 K at 180.3 and 182.3 GHz, respectively. While the decrease in UD's BT signature is 278 and 261 at the same frequencies, the slope of this decrease turns out to be strongly dependent on the size and concentrations of the ice particles. However, that itself becomes the signatures to distinguish UM and UD, because the curves show cross over ($BT(89\text{ and }150)_{LM} < BT(89\text{ and }150)_{UM}$ and $(BT(89\text{ and }150)_{UD} < BT(89\text{ and }150)_{CS}$, whereas $BT(180\text{ and }182)_{LM} > BT(180\text{ and }182)_{UM}$ and $BT(180\text{ and }182)_{UD} > BT(180\text{ and }182)_{CS}$).

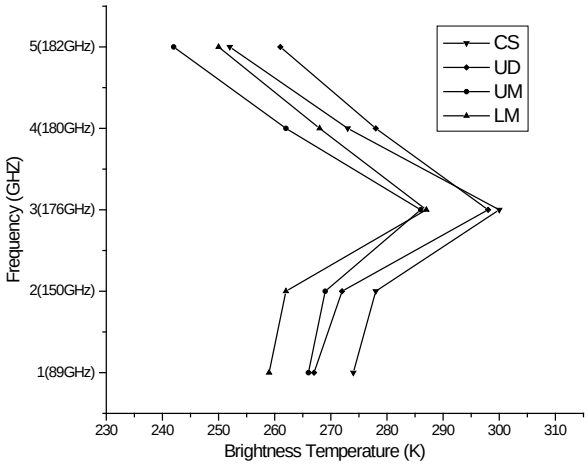

Figure 7. The average values of BT as a function of channel-frequency for events in Class III: CS, UD, and UM along with LM as a reference.

7 Discussion

Precipitating and non-precipitating hydrometers have different ΔBT, defined according to Eq. (1), for successive frequencies, particularly for 89 and 150 GHz. The signatures of the above mentioned three classes, in AMSU-B data,

are described and discussed in more details in the following. For simplicity and better understanding of similarities and dissimilarities between the classes, the differences between average BT values for two successive frequency channels ν_1 and ν_2, which may be more useful for our classification, are defined by Eq. (1):

$$\Delta BT(\nu_1,\nu_2) = BT(\nu_1) - BT(\nu_2) \qquad (1)$$

Table 4 shows the calculated values of $\Delta BT(\nu_1,\nu_2)$ for all types of hydrometeors referred to in Table 1.

The calculated differences (slopes) in Table 4 clearly show that:

1. The value of $\Delta BT(150,89)$ is negative for all precipitating hydrometers whereas it is positive for non-precipitating hydrometers.

2. The negative value of $\Delta BT(150,89)$ increases as the intensity and size of the droplets in precipitating hydrometers increase, i.e. the 150 GHz frequency is more sensitive to water droplet, due to scattering, and its corresponding BT becomes ever colder from LR to TS.

3) $\Delta BT(176,150)$ values are positive for all precipitating and non-precipitating hydrometeors. Maximum and minimum values are related to SC and TS respectively; i.e. the rain cannot be shown in the 176 GHz frequency because its weighting function peaks at higher altitudes which are generally above the rain layer except for convective thunderstorms which are extended to higher levels. On the other hand, the 150 GHz frequency peaks at around 2 to 3 km altitudes where most of the large rain droplets and ice crystals exist and cause

Table 4. The calculated average differential BT values, between two successive frequency channels of ν_1 and ν_2, for all precipitating and non-precipitating hydrometeors in Table 1.

$\Delta T_B(\nu_1,\nu_2)$	CS	SC	UD	UM	LM	LR	MR	SF	HR	TS
$\Delta T_B(150,89)$	+4	+7	+5	+3	+3	-1	-5	-4	-23	-29
$\Delta T_B(176,150)$	+22	+37	+26	+17	+25	+20	+20	+26	+30	+12
$\Delta T_B(180,176)$	-27	-10	-20	-24	-19	-17	-13	-16	+1	+5
$\Delta T_B(182,180)$	-21	-16	-17	-20	-18	-15	-15	-14	-13	+12

more scattering. It is to be noted that when the rain intensity increases, there is an increase in the value of $\Delta BT(176,150)$ up to some maximum (30 for HR and after that, it decreases (for TS).

4) Examining the third and fourth rows in Table 4 reveals that the responses of all three water vapor channels to cloud (UD, LM), rain (LR, MR), ice crystals (UM) and snowfall (SF) give negative values of $\Delta BT(182,180)$ and $\Delta BT(180,176)$ (except for HR & TS). The response of water vapor channels to heavy precipitating hydrometeors like HR and TS give positive values of $\Delta BT(180,176)$, whereas the $\Delta BT(182,180)$ has a negative value for HR and a positive value for TS.

8. A case study

We selected a day during which thunderstorm and rain were reported (07 December 2001 at 2300 GMT). The BT values of 5 AMSU-B channels for a scan line, which crossed through the thunderstorm, were calculated. The AMSU-B TB images of two window channels for 07 December at 2250 GMT shown in Figure 8 represent the selected scan line. Figure 9 shows the AMSU-B BT measurements at all five frequencies along the scan line, from A (30.82 N, 46.67 E) to B (29.67 N, 55 E).

As can be seen, the scan line crosses through the center of the thunderstorm that was reported for Ahwaz on 07 December at 2300 GMT. Note that Ahwaz is located slightly north of the Persian Gulf (Figure 1) and therefore, the selected scan line does not cross the Persian Gulf.

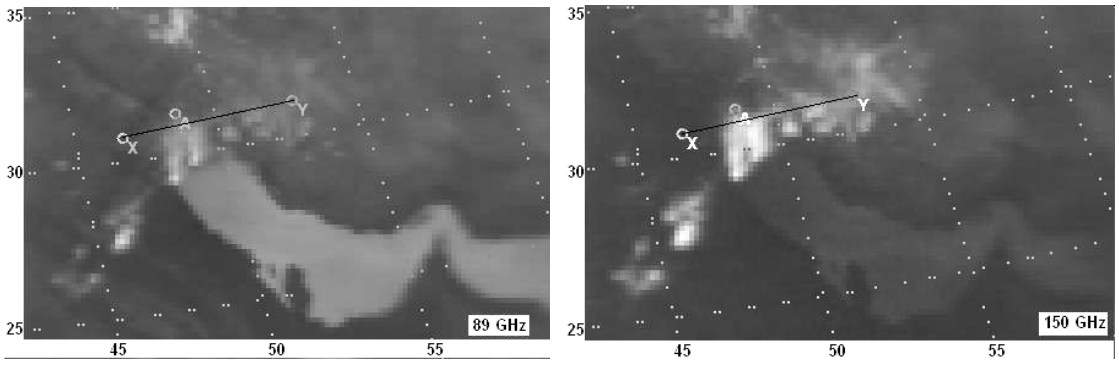

(a) **(b)**

Figure 8. AMSU-B BT images for 07 December 2001 at 2251 GMT, (a) 89 GHz and (b) 150 GHz. Location of the Ahwaz Station, where thunderstorm was reported at 2300 GMT is indicated with capital letter "A", between x and y points.

It is clear from Figure 9 that all BT curves show a minimum in the longitude corresponding to TS location around Ahwaz. However, the lowest and the highest BT depression values are around 63 K and 115 K, which occurred at 89 and 150 GHz, respectively. As mentioned earlier, this is due to the fact that the 150 GHz frequency is more sensitive to ice particles and water droplets and has large scattering parameters in comparison with 89 GHz (Muller et al. 1994). The times of the synoptic report for TS and the AMSU-B passes in the case considered here were 10 minutes different, which is perhaps the cause of non-coincidence between the location of the highest TB depression (49.3 E) and the longitude of the Ahwaz station (48.72 E) seen in Figure 9. However, large ice particles must have been present near the center of TS and must have produced a large amount of rainfall, over a much wider area. As noted earlier in Section 5, the area around 46.6 E to 47.8 E, with BT values of about 265, and 273 K at 89 and 150 GHz, respectively, shows the clear sky condition. At 52.3 E, the BT value had decreased to a value of around 244 K for channels 89 and 150 GHz, and hence it appeared to be one more rainy area that did not coincide with a reporting station. As BT values at 176 as well as 180 GHz had relative minima corresponding to 270 and 253 K, respectively, by comparing these conditions with those in Figure 3, one can tell that it is the signature of a cold heavy rain region. Moreover, the 182 GHz frequency was not contaminated by the heavy rain area and thus the rainy area was extended only up to about 7 - 8 km altitudes. The area around 53.3 E to 53.9 E showed a small relative minimum in BT at lower frequencies (89 and 150 GHz), and hence it may indicate the signature of warm or light rain (warm rain refers to a rain without ice layer aloft). Therefore, the water vapor channels, which are weighted above 700 hPa, cannot detect the warm rain regions.

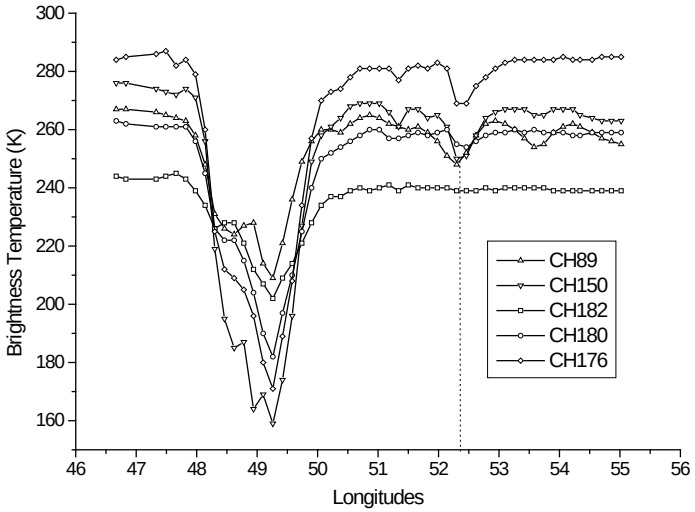

Figure 9. BT curves for five AMSU-B channels across thunderstorm, which was reported from Ahwaz (31.28 N, 48.72 E) on 07 December 2001 at 2300 GMT.

9 Conclusions

The results of quantitative measurements of BT suggest that the signatures of different types of hydrometeors are sufficiently reliable. The distinguishing points for this type of analysis are: (a) the value of BT at 89 GHz, (b) slopes of BT curves between 89 and 150 GHz, (c) a crossover of BT curves at 183 GHz with respect to 89 GHz and (d) different ΔBT, defined according to Eq. (1), for successive frequencies particularly for 89 and 150 GHz. Different meteorological situations are seen to be divided into three main classes: (I) The events with quite a low BT at all AMSU-B frequencies, which are related to heavy precipitating hydrometeors (TS and HR) and quite low a BT at 89 GHz, which are related to snow cover; (II) All low and moderate precipitating hydrometeors (LR, MR and SF) show a decrease in average BT between 89 and 150 GHz; and (III) All non-precipitating hydrometeors (moisture and clouds at different altitudes) show a rise in BT between 89 and 150 GHz. (IV) One main distinguishing point is that the precipitating and non-precipitating hydrometers have different ΔBT values defined according to Eq. (1) for successive frequencies particularly for 89 and 150 GHz. We believe that the classification of the hydrometeors using the microwave radiometer data from AMSU provides new inputs to the scientists working in the field of Atmospheric Sciences. It is thus felt that using these quantitative signatures one can "remotely see" the present weather situation anywhere at meso-scale, and hence they can be of help for "operational forecasters" for their predictions, and serve as a useful tool for air traffic planning purposes.

Acknowledgments

We are grateful to Hormozgan University and I. R. of Iran Meteorological Organization for supporting this work. The visible and infrared image data were taken from METOSAT satellite (University of Dundee, UK), and the microwave level 1b data from AMSU-B was obtained from the Comprehensive Large Array-data Stewardship System (CLASS) of US National Oceanic and Atmospheric Administration (NOAA).

References

Bennartz, R., and Petty, G. W., 2001, The sensitivity of microwave remote sensing observations of precipitation to ice particle size distribution: J. Appl. Meteor., **40**, 345-364.

Ferraro, R., Weng, F., Grody, N. C., Zhao, L., 2000, Precipitation characteristics over and from the NOAA-15 AMSU sensor: Geophys. Res. Letter, **27**, 2669-2672.

Grody, N. C., Zhao, J., Ferraro, R., Weng, F., and Boers, R., 2001, Determination of perceptible water and cloud liquid water over Ocean from NOAA 15 advanced microwave sounding unit: J. Geophys. Res., **106**, 2943-2953.

Katsumata, M., Uyeda, H., Iwanami, K., and Liu, G., 2000, The response of 36 and 89GHz microwave channels to convective snow clouds over Ocean: observation and modeling: J. Appl. Meteor., **39**, 2322-2335.

Kidder, S. Q., Goldberg, M. D., Zehr, R. M., Demana, M., Purdom, T. F., Velden C. S., Grody, N., and Kusselson, S. J., 2000, Satellite analysis of tropical cyclones using the advanced microwave

sounding unit (AMSU): Bull. Am. Meteor. Soc., **81**, 1241-1259.

Large Array-data Stewardship System (CLASS), available online at http://www.class.noaa.gov

Liu, G., and Curry, J. A., 1996, Large-scale cloud features during January 1993 in the North Atlantic Ocean as determined from SSM/I and SSM/T2: J. Geophys. Res., **101**, 7019-7032.

Liu, G., and Curry, J. A., 1997, Precipitation characteristics in Greenland-Iceland-Norwegian Seas determined by using satellite microwave data: J. Geophys. Res., **102**, 13987-13997.

METEOSAT images available online at: http://www.sat.dundee.ac.uk

Muller, B. M., Henry, E. F., and Xiang, X., 1994, Simulations of the effects of water vapor, cloud liquid water, and ice on AMSU moistures channel brightness temperatures: J. Appl. Meteorol., **33**, 1133-1154.

NOAA K L M User's Guide, available online at: http://www.2.ncdc.noaa.gov/docs/klm/

Saunders, R. W., Hewison, T. J., Stringer, S. J., and Atkinson, N. C., 1995, The radiometric characterization of AMSU-B: IEEE. Trans. on Microwave Theory and Techniques, **43**, 760-771.

Schools., J. L., Weinman, J. A., Alexander, G. D., Stewart, R. E., Angus, L. J., and Lee, C. L., 1999, Microwave properties of frozen precipitation around a North Atlantic Cyclone: J. Appl. Meteor., **38**, 29-43.

Staelin, D. H., and Chen, F. W., 2000, Precipitation observation near 54 and 183 GHz using the NOAA-15 satellite: IEEE Trans. on Geosciences and Remote sensing, **38**, 2322-2332.

Wang, J. R., Zhan, J., and Racette, P., 1997, Storm-associated microwave radiometric signatures in the frequency range of 90-220 GHz: J. Atmos. Oceanic Technology, **14**, 13-31.